ChemPubSoc Europe

DOI: 10.1002/ejoc.201701228

EurJOC European Journal of Organic Chemistry

Full Paper

Nanoparticles | *Very Important Paper* |

VIP

Preparation of Well-Ordered Mesoporous-Silica-Supported Ruthenium Nanoparticles for Highly Selective Reduction of Functionalized Nitroarenes through Transfer Hydrogenation

Ning Wei,[a,b] Xiujing Zou,*[a,b] Haigen Huang,[a,b] Xueguang Wang,*[a,b] Weizhong Ding,[a,b] and Xionggang Lu[a,b]

Abstract: MCM-41-type mesoporous silica (OMS-IL) was prepared by using an ionic liquid (1-hexadecyl-3-methylimidazolium bromide) as a template. The XRD and TEM results demonstrated that OMS-IL was more stable than the MCM-41 material. Ru nanoparticles were supported on OMS-IL (Ru/OMS-IL) by impregnating OMS-IL with a $RuCl_3$ aqueous solution, and the resulting material was used for the selective reduction of nitroarenes. The effects of the components of the catalysts and the reaction conditions on the catalytic behavior of the prepared catalysts were investigated in detail. Ru/OMS-IL exhibited high catalytic activity and chemoselectivity for the reduction of various substituted nitroarenes to the corresponding aromatic amines in ethanol with hydrazine hydrate as a hydrogen donor under mild conditions. The Ru/OMS-IL catalysts were highly stable and could easily be recovered by simple filtration over at least six recycling reactions without any observable loss in catalytic performance.

Introduction

Functionalized aromatic amines are important intermediates in the production of a range of pharmaceuticals, agrochemicals, cosmetics, herbicides, dyes, and polymers.[1–4] Amines can be obtained through the catalytic hydrogenation of the corresponding aromatic nitro compounds by using reducing agents such as hydrosilanes,[5] sodium borohydride,[6] hydrazine derivatives,[7,8] formic acid,[9] and molecular hydrogen.[10,11] However, selectivity in the targeted reduction of the $-NO_2$ group in the presence of other reactive function groups (e.g., alkenes, nitriles, esters, and halogen groups) remains a big challenge for the production of aromatic amines.[12] Homogeneous metal catalysts, especially Ru and Ir complexes, are usually used for the catalytic hydrogenation of nitro compounds.[13–15] However, the homogeneous catalytic process is generally unaccepted as a preferential alternative, as recovery and reuse of the expensive metals are difficult and most of the reactions do not proceed without the use of expensive ligands. Heterogeneous catalysts (noble metal catalysts such as Au,[1,16,17] Pd,[18–21] Pt,[22,23] and Ru[13,25,26]) have many advantages over their homogeneous counterparts, including easy removal from reaction mixtures and recyclability. Ru catalysts, especially those supported on high-surface-area heterogeneous catalyst supports, are recognized as promising catalysts for the catalytic hydrogenation of nitro compounds because of their high catalytic activity and low cost.[15,25,26] So, it is a challenge to develop cost-effective and highly efficient heterogeneous noble-metal catalysts for the green chemoselective reduction of nitroarenes.

It is generally believed that the high surface area of heterogeneous catalysts results in their high catalytic activity. The mesoporous material MCM-41 is a good candidate for a solid support, as it has a regular pore diameter of ca. 5 nm and a high surface area (> 1000 $m^2 g^{-1}$).[27] Its large pore size allows the passage of large molecules such as organic reactants and metal complexes through the pores so that they may reach the surfaces of the channels.[28–30] Nevertheless, MCM-41 is reported to have high thermal stability and hydrothermal stability in air and oxygen-containing water vapor. However, it has low hydrothermal stability in water and aqueous solutions.[31,32] To enlarge the application range of MCM-41, it is important to improve its hydrothermal stability.[33] It was reported that by adapting the synthesis parameters, such as the type of silicium source, type of template, pH, and temperature, different materials could be synthesized with varying porosity and crystallinity.[32]

In the present study, ordered mesoporous silica (OMS-IL) with good hydrothermal stability was synthesized by using 1-hexadecyl-3-methylimidazolium bromide (C_{16}mimBr) as a template. OMS-IL-supported Ru catalysts (Ru/OMS-IL) were prepared by the impregnation method. Ru species were uniformly dispersed in the mesoporous silica without changes in the ordered mesoporous structure. Their behavior in the reduction of nitroarenes to the corresponding aromatic amines with hydra-

[a] *State Key Laboratory of Advanced Special Steel, Shanghai University Shanghai 200072, China*
[b] *Shanghai Key Laboratory of Advanced Ferrometallurgy, School of Materials Science and Engineering, Shanghai University, Shanghai 200072, China*
E-mail: xjzou@shu.edu.cn
wxg228@shu.edu.cn
http://www.sklass.shu.edu.cn/

Supporting information for this article is available on the WWW under https://doi.org/10.1002/ejoc.201701228.

zine hydrate (N_2H_4•H_2O) in ethanol without any other additive (acid or base) was intensively investigated. The Ru/OMS-IL catalysts exhibited excellent catalytic activity and chemoselectivity for the reduction of nitroarenes to the corresponding aromatic amines. Noticeably, hydrazine hydrate as a hydrogen donor generated only N_2 as a byproduct.

Results and Discussion

Physical and Chemical Properties of the Catalysts

XRD was first used to study the crystalline phases of the prepared materials. Figure 1 displays the small- and wide-angle XRD patterns of the prepared samples. The results of the small-angle XRD patterns (Figure 1a) show that both MCM-41 materials prepared possess a strong diffraction peak at around 2θ = 2.1–2.4° and two other weak peaks at 2θ = 3.7–4.1 and 4.3–4.8°, which can be assigned to the lattice faces (100), (110), and (200), respectively, indicating a quasiregular arrangement of the mesopores with hexagonal symmetry.[35] Relative to the diffraction peaks of MCM-41 in Figure 1, the diffraction peaks representing the ordered mesoporous structure of OMS-IL are shifted to smaller angles. This indicates that the pore walls are thicker in the OMS-IL samples than in MCM-41[36] likely as a result of C_{16}mimBr (used as a template) having longer molecular chains than cetyltrimethylammonium bromide (CTAB). For 0.5Ru/MCM-41, the intensity of the diffraction deceases gradually relative to that of MCM-41, which indicates that the initially ordered pore channels of MCM-41 are destroyed once Ru is supported. In the case of the 0.5Ru/OMS sample, there are also clear diffractions at 2θ = 2.4, 4.1, and 4.8°, and the intensities of the diffractions do not change distinctly relative to those of the OMS-IL support, which indicates that the quasiregular arrangement of the mesopores with hexagonal symmetry is not destroyed after supporting Ru by using the impregnation method. It is speculated that the good stability of OMS-IL can be attributed to thicker pore walls, as reported previously.[37,38] The wide-angle XRD patterns of all the samples in Figure 1b show typical broad bands for the amorphous silica walls of solid mesoporous MCM-41. Diffraction peaks for Ru species are not observed in the 0.5Ru/MCM-41 and 0.5Ru/OMS-IL samples, which indicates that Ru is highly dispersed in these mesomaterials. These results are consistent with the TEM observations (Figure 2). The TEM images show that the pore walls are thicker in the OMS-IL sample than in MCM-41, which is in accordance with the XRD results. Considering the indiscernible Ru particle size in 0.5Ru/OMS-IL, Ru/OMS-IL samples with higher Ru loading were prepared and characterized by TEM. Figure 3 shows that for all of the *x*Ru/OMS-IL samples (*x* = 1, 2, and 3), ultrafine, dark Ru nanoparticles are homogeneously distributed throughout the silica matrices. The size of the Ru nanoparticle increases slightly upon increasing the Ru loading.

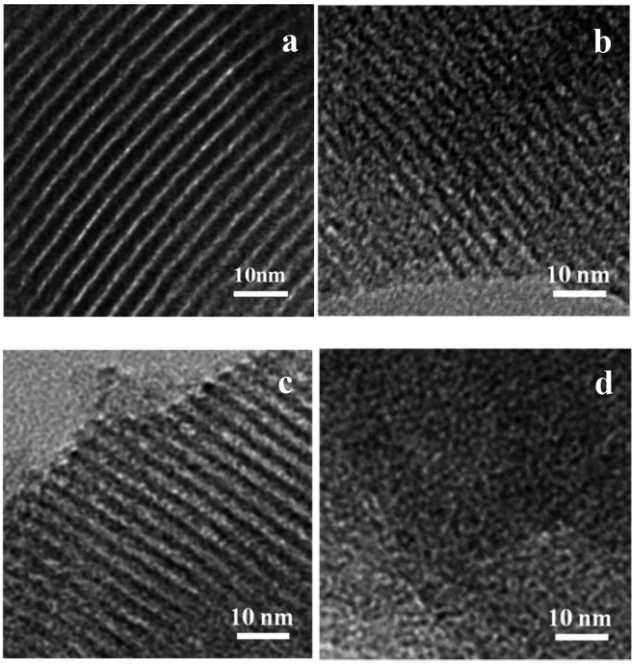

Figure 2. TEM images of the prepared samples: (a) OMS-IL, (b) MCM-41, (c) Ru/OMS-IL, and (d) Ru/MCM-41.

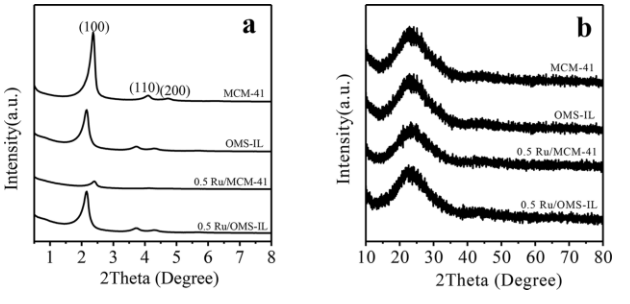

Figure 1. (a) Low-angle and (b) wide-angle XRD patterns of the prepared samples.

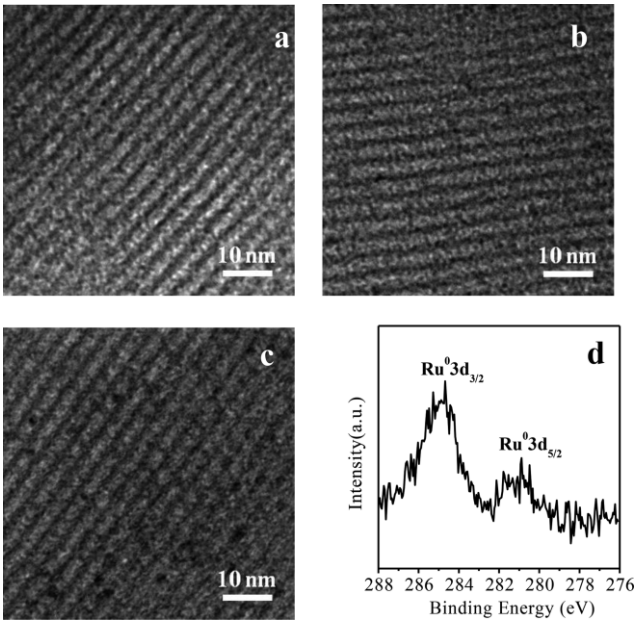

Figure 3. TEM images of (a) 1Ru/OMS-IL, (b) 2Ru/OMS-IL, and (c) 3Ru/OMS-IL. (d) X-ray photoelectron spectrum of 0.5Ru/OMS-IL.

The Ru X-ray photoelectron spectrum (Figure 3d) of 0.5Ru/OMS-IL shows that the Ru 3d spectral bands at binding energies (BEs) of 284.4 and 280.2 eV are dominant, and they can be attributed to Ru^0;[26] they indicate that metallic Ru is formed as the major phase on the surfaces. BJH analysis (not shown) indicates that both OMS-IL and MCM-41 present uniform pore-size distributions. Table 1 displays the textural properties of the prepared materials. Compared with the MCM-41 support, 0.5Ru/MCM-41 exhibits a clear decrease in the BET surface area, pore volume, and pore size. MCM-41 shows a specific surface area (S_{BET}) of 1242 $m^2 g^{-1}$, a pore volume (V_p) of 0.90 $cm^3 g^{-1}$, and a pore size (D_p) of 2.9 nm, whereas those of 0.5Ru/MCM-41 are 771 $m^2 g^{-1}$, 0.47 $cm^3 g^{-1}$, and 2.4 nm, respectively. These results may be related to destruction of the initial ordered pore channels of MCM-41. Compared with OMS-IL, 0.5Ru/OMS-IL has a smaller specific surface area, pore volume, and average pore size owing to partial coating of the OMS-IL surface by Ru and variation in the mass density of the catalysts.

Table 1. Textural properties of the prepared materials.

Sample	S_{BET} [$m^2 g^{-1}$]	V_p [$cm^3 g^{-1}$]	D_p [nm]
MCM-41	1242	0.90	2.9
OMS-IL	1051	1.03	3.9
0.5Ru/MCM-41	771	0.47	2.4
0.5Ru/OMS-IL	940	0.85	3.6

Catalytic Reaction

The reduction of 4-methoxylnitrobenzene was examined as a model reaction over the prepared catalysts to optimize the components of the samples, and the results are shown in Table 2. Ru catalysts with various supports were prepared, and their catalytic performances were evaluated (Table 2, entries 1–8). Both of the SiO_2-supported Ru catalysts presented much

Table 2. Performance of the prepared catalysts for the chemoselective reduction of 4-methoxynitrobenzene to 4-methoxyaniline.[a].

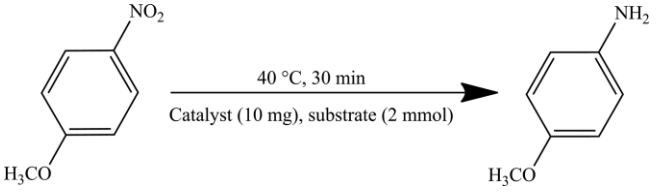

Entry	Catalyst	Reducing agent [equiv.]	Solvent [mL]	Conversion [%]	Selectivity [%]
1	0.5Ru/OMS-IL	N_2H_4 (6)	EtOH (2)	69	>99
2	0.5Ru/MCM41	N_2H_4 (6)	EtOH (2)	28	>99
3	0.5Ru/SBA-15	N_2H_4 (6)	EtOH (2)	32	>99
4	0.5Ru/C	N_2H_4 (6)	EtOH (2)	8	>99
5	0.5Ru/TiO_2	N_2H_4 (6)	EtOH (2)	5	>99
6	0.5Ru/Al_2O_3	N_2H_4 (6)	EtOH (2)	4	>99
7	0.5Ru/CeO_2	N_2H_4 (6)	EtOH (2)	<1	–
8	0.5Ru/ZrO_2	N_2H_4 (6)	EtOH (2)	<1	–
9	0.5Au/OMS-IL	N_2H_4 (6)	EtOH (2)	<1	–
10	0.5Ag/OMS-IL	N_2H_4 (6)	EtOH (2)	3	>99
11	0.5Pt/OMS-IL	N_2H_4 (6)	EtOH (2)	22	>99
12	0.5Pd/OMS-IL	N_2H_4 (6)	EtOH (2)	17	>99
13[b]	0.25Ru/OMS-IL	N_2H_4 (6)	EtOH (2)	67	>99
14[c]	1.0Ru/OMS-IL	N_2H_4 (6)	EtOH (2)	57	>99
15[d]	2.0Ru/OMS-IL	N_2H_4 (6)	EtOH (2)	50	>99
16[e]	3.0Ru/OMS-IL	N_2H_4 (6)	EtOH (2)	41	>99
17	0.5Ru/OMS-IL	$NaBH_4$ (6)	EtOH (2)	36	64
18	0.5Ru/OMS-IL	HCOOH (6)	EtOH (2)	<1	–
19	0.5Ru/OMS-IL	HCOOK (6)	EtOH (2)	<1	–
20[f]	0.5Ru/OMS-IL	H_2	–	<1	–
21	0.5Ru/OMS-IL	N_2H_4 (0)	EtOH (2)	<1	–
22	0.5Ru/OMS-IL	N_2H_4 (2)	EtOH (2)	28	98
23	0.5Ru/OMS-IL	N_2H_4 (4)	EtOH (2)	59	>99
24	0.5Ru/OMS-IL	N_2H_4 (8)	EtOH (2)	71	>99
25	0.5Ru/OMS-IL	N_2H_4 (6)	iPrOH (2)	59	>99
26	0.5Ru/OMS-IL	N_2H_4 (6)	THF (2)	29	>99
27	0.5Ru/OMS-IL	N_2H_4 (6)	toluene (2)	43	>99
28	0.5Ru/OMS-IL	N_2H_4 (6)	EtOAc (2)	23	98
29	0.5Ru/OMS-IL	N_2H_4 (6)	distilled H_2O (2)	17	76
30	0.5Ru/OMS-IL	N_2H_4 (6)	EtOH (0)	52	>99
31	0.5Ru/OMS-IL	N_2H_4 (6)	EtOH (1)	60	>99
32	0.5Ru/OMS-IL	N_2H_4 (6)	EtOH (4)	43	>99
33	0.5Ru/OMS-IL	N_2H_4 (6)	EtOH (6)	32	>99

[a] Reaction conditions: catalyst (10 mg), 4-methoxynitrobenzene (2 mmol), 40 °C, 30 min. [b] Catalyst (20 mg). [c] Catalyst (5 mg). [d] Catalyst (2.5 mg). [e] Catalyst (1.7 mg). [f] P_{H_2} = 2 MPa.

higher conversions of 4-methoxynitrobenzene than all of the other support catalysts. Specifically, 0.5Ru/OMS-IL showed a much higher conversion of 4-methoxynitrobenzene (69 %) than the 0.5Ru/MCM-41 (28 %) and 0.5Ru/SBA-15 (32 %) samples. Although both OMS-IL and SBA-15 were hydrothermally stable, the excellent activity of 0.5Ru/OMS-IL might result from readily accessible and uniform catalytic sites within the appropriate pore structure of OMS-IL.[39] In the case of 0.5Ru/MCM-41, the collapsed structure led to aggregation of the ruthenium particles, and a decrease in the number of active sites was the main reason for the low reaction activity. The conversion of 4-methoxynitrobenzene was lower on the Au-, Ag-, Pt-, and Pd-supported OMS-IL catalysts (Table 2, entries 9–12) than on the 0.5Ru/OMS-IL catalyst. The effect of the Ru loading was investigated (Table 2, entries 1 and 13–16), and the highest conversion was obtained with 0.5Ru/OMS-IL. The effects of the hydrogen

Table 3. Chemoselective reduction of various nitroarenes over 0.5Ru/OMS-IL.[a]

Entry	Substrate	Time [h]	Conv. [%]	Sel. [%]	TOF[b] [h^{-1}]	Entry	Substrate	Time [h]	Conv. [%]	Sel. [%]	TOF[b] [h^{-1}]
1		0.5	> 99	> 99	42200	16	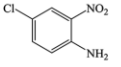	2	> 99	> 99	3800
2		0.5	> 99	> 99	7115	17	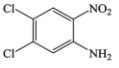	4	> 99	> 99	1989
3		0.5	> 99	> 99	8762	18	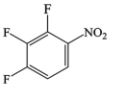	3	> 99	> 99	3069
4	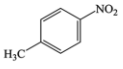	0.5	> 99	> 99	6666	19	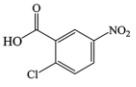	4	> 99	> 99	2127
5	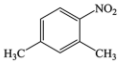	2	> 99	> 99	4080	20	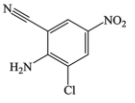	4	> 99	> 99	2578
6	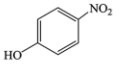	6	94	> 99	1911	21	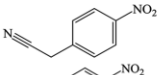	10	> 99	> 99	1251
7	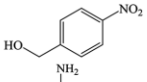	2	100	> 99	3569	22	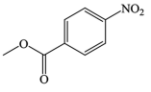	1	> 99	> 99	15926
8	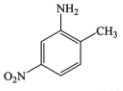	1	> 99	> 99	5618	23	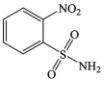	1	> 99	> 99	10644
9	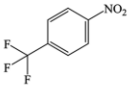	2	> 99	> 99	3653	24	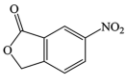	4	> 99	> 99	2406
10		0.5	> 99	> 99	20832	25[c]	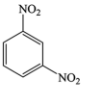	2	> 99	> 99	4224
11		0.5	> 99	> 99	31152	26[d]	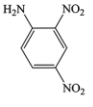	3	> 99	> 99	2932
12	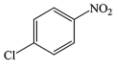	0.5	> 99	> 99	15572	27		4	> 99	> 99	1677
13	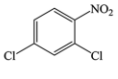	1	> 99	> 99	17336	28		3	> 99	> 99	7137
14	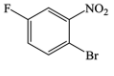	1	> 99	> 99	21056	29		2	> 99	> 99	5068
15	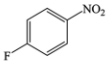	1	> 99	> 99	7186	30		2	> 99	> 99	4721

[a] Reaction conditions: catalyst (10 mg), 4-methoxylnitrobenzene (2 mmol), $N_2H_4{\cdot}H_2O$ (12 mmol), ethanol (2 mL), 40 °C. [b] TOF: turnover frequency; calculated on the basis of total metal and substrate conversions at 10 %. [c] The product was 1,2,4-benzenetriamine. [d] The product was 1,3-diaminobenzene.

donor, solvent, and substrate concentration were investigated in detail to optimize the reaction conditions, and the results are summarized in Table 2 (entries 17–33). Initially, we explored the reduction of 4-methoxynitrobenzene in the presence of 0.5Ru/OMS-IL with five different hydrogen donors: hydrazine hydrate, sodium borohydride, formic acid, potassium formate, and hydrogen (Table 2, entries 17–21). The use of hydrazine hydrate (Table 2, entry 1) in ethanol as the solvent resulted in the highest conversion of 4-methoxynitrobenzene (69 %) with >99 % selectivity to 4-methoxyaniline. Upon using sodium borohydride in ethanol, the conversion of 4-methoxynitrobenzene was 36 % and the selectivity to 4-methoxyaniline was 64 %. The use of formic acid or potassium formate in ethanol or hydrogen as the hydrogen donor did not show any conversion. The catalytic activity increased upon increasing the hydrazine content and approached a stable value if the molar ratio of hydrazine to substrate reached 6:1 (Table 2, entries 1 and 22–24); all of the solvents, including ethanol, isopropyl alcohol, THF, toluene, ethyl acetate, and distilled water, resulted in excellent catalytic performances, but ethanol [4-methoxynitrobenzene/ethanol = 2:1 (mmol mL^{-1})] allowed the highest conversion of 4-methoxynitrobenzene (Table 2, entries 1 and 25–33).

The selective hydrogenation protocol of the 0.5Ru/OMS-IL catalyst was further extended to the conversion of various substituted nitroarenes into the corresponding amines to demonstrate the generality of this reaction under the optimized conditions, and the results are summarized in Table 3. 0.5Ru/OMS-IL presented high intrinsic activity and excellent selectivity in the hydrogenation reactions to the corresponding aromatic amines under the given conditions. Nitroarenes with nonreducible groups such as $–CH_3$, –OH, $–NH_2$, and $–CF_3$ (Table 3, entries 1–9), were quantitatively transformed into the corresponding amines in yields >99 %. Furthermore, we were pleased to find that halo (F, Cl, Br)-substituted nitroarenes could be reduced to the corresponding anilines with no discernible dehalogenation (Table 3, entries 10–20). A number of other reducible functional groups (e.g., carboxy, ester, nitrile, amide, and sulfanilamide) were tolerated in the reduction reaction (Table 3, entries 21–24). Notably, dinitrobenzenes were reduced to the corresponding diaminobenzenes (Table 3, entries 25 and 26). Interestingly, chemoselective reduction of N-heterocyclic nitroarenes could also be performed to give the corresponding amines in yields >99 % (Table 3, entries 27–30). In these reactions, sufficiently high chemoselectivity for reduction of the nitro group in the benzene ring can likely be attributed to the fact that the nitro group is more reactive than other reducible groups over the catalyst, and this is strongly supported by intermolecular competitive reductions that were performed separately. Upon reducing mixtures of nitrobenzene and other reducible-group-substituted benzenes (e.g., benzoic acid, ethyl benzoate, benzonitrile, benzamide, styrene, quinoline) with hydrazine in ethanol at 40 °C, nitrobenzene was completely converted into aniline, whereas the other reactants did no undergo any reaction. These results indicate that the 0.5Ru/OMS-IL catalyst has both high activity and high selectivity for the chemoselective reduction of various functionalized nitroarenes under mild conditions.

To investigate the reusability of the 0.5Ru/OMS-IL catalyst for the chemoselective reduction of nitroarenes, the selective reduction of 2,4-dichloronitrobenzene was examined as an example. The selective reduction of 2,4-dichloronitrobenzene with ca. 74 % conversion in the first cycle (Figure 4), at which the reduction of 2,4-dichloronitrobenzene was controlled by chemical kinetics, was evaluated under the optimum conditions. After every run, the catalyst was recovered by simple filtration, which was followed by washing with ethanol. The conversion of 2,4-dichloronitrobenzene decreased only slightly from 75 to 65 % after six cycles, whereas the selectivity to 2,4-dichloroaniline was maintained at >99 % (Figure 3). After the sixth run, the spent catalyst was characterized by XRD. No observable changes in the ordered mesoporous structure or Ru particle size were detected. Inductively coupled plasma atomic emission spectrometry (ICP-AES) analyses showed that the amount of Ru in the filtrate was negligible (< 1 ppm), which indicated that leaching of the metal components did not occur during the reaction procedure.

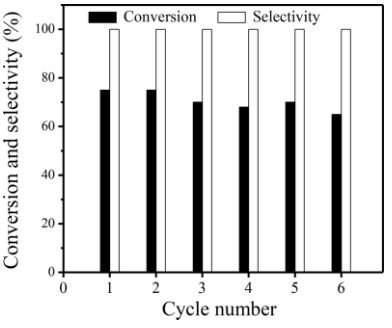

Figure 4. Reusable profiles of the 0.5Ru/OMS-IL catalyst for the selective reduction of 2.4-dichloronitrobenzene to 2,4-dichloroaniline. Reaction conditions: catalyst (20 mg), 2,4-dichloronitrobenzene (4 mmol), $N_2H_4{\cdot}H_2O$ (24 mmol), ethanol (3 mL), 40 °C.

Conclusions

In summary, OMS-IL- with stable structures was prepared by using 1-hexadecyl-3-methylimidazolium bromide as a template. The Ru/OMS-IL catalysts, prepared by the impregnation method, efficiently and quantitatively reduced various functionalized nitroarenes to the corresponding anilines with yields >99 % by using hydrazine hydrate. Recycling tests and characterization revealed that 0.5Ru/OMS-IL was highly stable and could be reused for the reduction of nitroarenes.

Supporting Information: Complete experimental details, characterization data.

Acknowledgments

This research was supported by the Open Project of the State Key Laboratory of Advanced Special Steel of Shanghai University (SKLASS2015-Z052), National Basic Research Program of China (973 Program, No. 2014CB643403), the National Natural Science Foundation of China (No. 51574164), and Basic Major Research Program of Science and Technology Commission Foundation of Shanghai (No. 14JC1491400).

Keywords: Ordered mesoporous silica · Ruthenium · Reduction · Nanoparticles · Nitroarenes

[1] D. Wang, D. Astruc, *Chem. Rev.* **2015**, *115*, 6621–6686.
[2] P. Lara, K. Philippot, *Catal. Sci. Technol.* **2014**, *4*, 2445–2465.
[3] S. Gladiali, E. Alberico, *Chem. Soc. Rev.* **2006**, *35*, 226–236.
[4] P. Serna, A. Corma, *ACS Catal.* **2015**, *5*, 7114–7121.
[5] D. Porwal, M. Oestreich, *Eur. J. Org. Chem.* **2016**, 3307–3309.
[6] P. Zhou, D. Li, S. Jin, S. Chen, Z. Zhang, *Int. J. Hydrogen Energy* **2016**, *41*, 15218–15224.
[7] H. Sun, Y. Ai, D. Li, Z. Tang, Z. Shao, Q. Liang, *Chem. Eng. J.* **2017**, *314*, 328–335.
[8] H. Huang, X. Wang, X. Li, C. Chen, X. Zou, W. Ding, X. Lu, *Green Chem.* **2017**, *19*, 809–815.
[9] L. Gong, Y. Cai, X. Li, Y. Zhang, J. Sun, J. Chen, *Green Chem.* **2014**, *16*, 3746–3751.
[10] Z. Shao, S. Fu, M. Wei, S. Zhou, Q. Liu, *Angew. Chem. Int. Ed.* **2016**, *55*, 14653–14657; *Angew. Chem.* **2016**, *128*, 14873–14877.
[11] S. Furukawa, K. Takahashi, T. Komatsu, *Chem. Sci.* **2016**, *7*, 4476–4484.
[12] C. Jiang, Z. Shang, X. Liang, *ACS Catal.* **2015**, *5*, 4814–4818.
[13] N. Marozsán, H. Horváth, A. Erdei, F. Joó, *J. Mol. Catal. A* **2016**, *425*, 103–109.
[14] P. P. Sarmah, D. K. Dutta, *Appl. Catal. A* **2014**, *470*, 355–360.
[15] P. Kluson, L. Cerveny, *Appl. Catal. A* **1995**, *128*, 13–31.
[16] N. Perret, X. Wang, T. Onfroy, C. Calers, M. A. Keane, *J. Catal.* **2014**, *309*, 333–342.
[17] W. Guo, R. Pleixats, A. Shafir, *Chem. Asian J.* **2015**, *10*, 2437–2443.
[18] J. Tuteja, S. Nishimura, K. Ebitani, *RSC Adv.* **2014**, *4*, 38241–38249.
[19] M. Vilches-Herrera, S. Werkmeister, K. Junge, A. Börner, M. Beller, *Catal. Sci. Technol.* **2014**, *4*, 629–632.
[20] D. Zhang, F. Ye, T. Xue, Y. Guan, Y. Wang, *Catal. Today* **2014**, *234*, 133–138.
[21] Y. Lu, H. Zhu, W. Li, B. Hu, S. Yu, *J. Mater. Chem. A* **2013**, *1*, 3783–3788.
[22] L. Cisneros, P. Serna, A. Corma, *Angew. Chem. Int. Ed.* **2014**, *53*, 9306–9310; *Angew. Chem.* **2014**, *126*, 9460–9464.
[23] S. Byun, Y. Song, B. M. Kim, *ACS Appl. Mater. Interfaces* **2016**, *8*, 14637–14647.
[24] A. J. A. Watson, A. J. Fairbanks, *Eur. J. Org. Chem.* **2013**, 6784–6788.
[25] R. B. N. Baig, R. S. Varma, *ACS Sustainable Chem. Eng.* **2013**, *1*, 805–809.
[26] Y. Gao, S. Jaenicke, G. Chuah, *Appl. Catal. A* **2014**, *484*, 51–58.
[27] J. S. Beck, J. C. Vartuli, W. J. Roth, M. E. Leonowicz, C. T. Kresge, K. D. Schmitt, C. T.-W. Chu, D. H. Olson, E. W. Sheppard, S. B. McCullen, J. B. Higgins, J. L. Schlenker, *J. Am. Chem. Soc.* **1992**, *114*, 10834–10843.
[28] T. Maschmeyer, F. Rey, G. Sankar, J. M. Thomas, *Nature* **1995**, *378*, 159.
[29] C. J. Liu, S. G. Li, W. Q. Pang, C. M. Che, *Chem. Commun.* **1997**, 2397–2398.
[30] W. Zhou, J. M. Thomas, D. S. Shephard, B. F. G. Johnson, D. Ozkaya, T. Maschmeyer, R. G. Bell, Q. Ge, *Science* **1998**, *280*, 705–708.
[31] R. Ryoo, S. Jun, *J. Phys. Chem. B* **1997**, *101*, 317–320.
[32] T. Linssen, K. Cassiers, P. Cool, E. F. Vansant, *Adv. Colloid Interface Sci.* **2003**, *103*, 121–147.
[33] J. R. Dodson, E. C. Cooper, A. J. Hunt, A. Matharu, J. Cole, A. Minihan, J. H. Clark, D. J. Macquarrie, *Green Chem.* **2013**, *15*, 1203–1210.
[34] C. T. Kresge, M. E. Leonowicz, W. J. Roth, J. C. Vartuli, J. S. Beck, *Nature* **1992**, *359*, 710–712.
[35] M. Zhang, W. Zhu, H. Li, S. Xun, W. Ding, J. Liu, Z. Zhao, Q. Wang, *Chem. Eng. J.* **2014**, *243*, 386–393.
[36] J. Qin, B. Li, W. Zhang, W. Lv, C. Han, J. Liu, *Microporous Mesoporous Mater.* **2015**, *208*, 181–187.
[37] R. Mokaya, *J. Phys. Chem. B* **1999**, *103*, 10204–10208.
[38] D. Das, C. Tsai, S. Cheng, *Chem. Commun.* **1999**, *5*, 473–474.
[39] C. del Pozo, A. Corma, M. Iglesias, F. Sanchez, *Green Chem.* **2011**, *13*, 2471–2481.

Received: September 4, 2017

